

Polymer Chemistry

Accepted Manuscript



This is an *Accepted Manuscript*, which has been through the Royal Society of Chemistry peer review process and has been accepted for publication.

Accepted Manuscripts are published online shortly after acceptance, before technical editing, formatting and proof reading. Using this free service, authors can make their results available to the community, in citable form, before we publish the edited article. We will replace this *Accepted Manuscript* with the edited and formatted *Advance Article* as soon as it is available.

You can find more information about *Accepted Manuscripts* in the [Information for Authors](#).

Please note that technical editing may introduce minor changes to the text and/or graphics, which may alter content. The journal's standard [Terms & Conditions](#) and the [Ethical guidelines](#) still apply. In no event shall the Royal Society of Chemistry be held responsible for any errors or omissions in this *Accepted Manuscript* or any consequences arising from the use of any information it contains.

ARTICLE

Complex Thermo-responsive Behavior of Diblock Polyacrylamides

Cite this: DOI: 10.1039/x0xx00000x

Yong-Guang Jia, X. X. Zhu*

Received 00th January 2012,
Accepted 00th January 2012

DOI: 10.1039/x0xx00000x

www.rsc.org/

Diblock thermo-responsive copolymers poly(*N*-*n*-propylacrylamide)-*b*-poly(*N*,*N*-ethylmethacrylamide) (PnPA-*b*-PEMA) of various block lengths were synthesized by a sequential reversible addition-fragmentation chain transfer (RAFT) polymerization. The work aims at the understanding of the complex thermo-responsive behavior of block copolymers whose aqueous solutions change, with increasing temperature, from a transparent solution, to a cloudy, and then to a clear and finally to turbid liquid. The thermo-responsive behavior depends on the polymer concentration and is reversible with a certain hysteresis. Dynamic light scattering and atomic force microscopy results help to assign the first cloud point to a transition from unimers to micellar clusters. The longer PnPA block relative to the PEMA block and the hydrogen bonding between the PnPA and PEMA blocks are determining forces for the formation of micellar clusters. Further rise in temperature leads to the restructuring and dissociation of these loose clusters into smaller micelles due to further dehydration of the PnPA block and the disruption of the hydrogen bonds between the PnPA and PEMA blocks, resulting in an optically clear solution. A second cloud point appears again when the micelles start to aggregate. A pseudo-phase diagram was obtained for the *N*-substituted polyacrylamides, providing guidelines towards the rational design of thermo-responsive copolymers showing two or more responsive temperatures.

Introduction

Thermo-responsive water-soluble polymers undergo phase transition in water from a soluble to an insoluble state when the temperature is above a certain point (lower critical solution temperature, LCST) or below a certain point (upper critical solution temperature, UCST).^{1,2} These polymers, especially those exhibiting the LCST behavior, have attracted a great deal of research interest in fields related to drug delivery, gene carriers, tissue engineering, sensors, catalysis, and chromatography separation in the past decades.³⁻¹¹ Block copolymers consisting of two or more different thermo-responsive blocks may exhibit two or more LCST-type transitions as each block undergo a transition from soluble to insoluble states at different temperatures.¹²⁻²¹ Some exhibited a sequential multi-stage collapse process of the blocks with increasing temperature.^{15-17,22} However, we have also observed that some of the block copolymers do not follow the regular step-wise aggregation as typically evidenced by the changes of turbidity of the aqueous solution. They change from a transparent, to cloudy at a certain cloud point (CP), then to clear and finally to turbid solution again during a heating. This may seem to be unusual, but has been observed for quite a number of polymers as reported in the literature.^{17,18,23,24} Hoogenboom et al recently have reported on copolymers of 2-ethyl-2-oxazoline (EtOx) and 2-*n*-propyl-2-oxazoline (PropOx),

PEtOx-*b*-P(EtOx-*s*-PropOx), which exhibited an intricate transmittance behavior whereby the samples upon heating became visually clear again after an initial CP and then exhibited a second CP at a higher temperatures. The dynamic light scattering (DLS) data indicated that the aggregates formed around the first CP restructured and fragmented into smaller micelle-like structures, causing the samples to become optically clear again.²⁴ The observed fragmentation was confirmed by the static light scattering (SLS) experiments. In an early study, Zhao et al also observed the formation of monodisperse, nearly spherical micelles between the two CPs in the intermediate temperature range, when an aqueous solution of poly(methoxytri(ethyleneglycol)acrylate)-*b*-poly(4-vinylbenzyl methoxytris (oxyethylene)ether) (1 wt%) was heated.²³ However, it is not clear what the driving force may be for the formation of the large aggregates around the first CP and how the large aggregates dissociate into smaller micelle-like structures.

Among the thermo-responsive polymers, poly(*N*-isopropyl acrylamide) (PiPA) is one of the most extensively studied.²⁵⁻²⁹ The phase transition temperature of related polyacrylamides may be tuned by varying the hydrophobicity of the *N*-substitution group on the monomers unit.^{14-17,30-33} In this work, we designed and synthesized thermo-responsive diblock PnPA-*b*-PEMA of varying block lengths. The CPs of the PnPA and PEMA blocks are different enough (22 and 56-57 °C,

respectively)^{34,35} and their aqueous solutions showed multiple transitions from transparent, to cloudy, to clear, and back to turbid solutions with increasing temperature. We attempt to elucidate the mechanism of the complex aggregation process and to understand the driving force using a combination of light scattering and microscopic techniques.

Experimental Section

Materials

All reagents were purchased from Aldrich and used without further purification unless otherwise stated. 2,2'-Azobisobutyronitrile (AIBN) was recrystallized twice from methanol. *N,N*-Ethylmethacrylamide (EMA) and *N*-*n*-propylacrylamide (nPA) were prepared from the corresponding alkylamine and acryloyl chloride as reported previously.³⁶ 2-Dodecylsulfanyliothiocarbonylsulfanyl-2-methyl propionic acid (DMP) was prepared according to a previously reported procedure³⁷ and used as the chain transfer agent (CTA) in the RAFT polymerization.

Synthesis of polymers

PnPA were prepared by a general RAFT polymerization method with AIBN as an initiator as described previously.¹⁷ Copolymerization was conducted in dimethyl sulfoxide (DMSO) at 70 °C with a [DMP]/[AIBN] ratio of 5. EMA (229.3 mg, 2.026 mmol), macro-CTA PnPA₈₄ (400.3 g, 0.0405 mmol), AIBN (1.32 mg, 0.008 mmol), and DMSO 4 mL were added to a 25 mL round-bottom flask. The mixture was purged with N₂ for 20 min prior to its immersion in a preheated oil bath at 70 °C. The copolymerization was allowed to proceed for 40 min before being quenched by immersion into ice-water. The reaction mixture was poured into cold ethyl ether. The precipitate was collected and dried *in vacuo* to yield 533 mg of PnPA₈₄-*b*-PEMA₄₂ (89.8%).

Polymer characterization

Size exclusion chromatography (SEC) was performed on a Breeze system from Waters equipped with a 717 plus autosampler, a 1525 Binary HPLC pump, and a 2410 refractive index detector using two consecutive Waters columns (Phenomenex, 5 μm, 300 mm × 7.8 mm; Styragel HR4, 5 μm, 300 mm × 7.8 mm). The eluent DMF containing 0.01 M LiBr was filtered through 0.2 μm nylon Millipore filters. The flow rate was 1 mL/min. Poly(methyl methacrylate) standards (2500-296 000 g/mol) were used for calibration. ¹H and ¹³C NMR spectra in CDCl₃ or D₂O were recorded on a Bruker AV400 spectrometer operating at 400 MHz for ¹H and 100 MHz for ¹³C. The cloud points (CPs) of the samples in aqueous solution were determined on a Cary 5000 UV-Vis-NIR spectrophotometer (Agilent) equipped with a Cary temperature controller. Polymer aqueous solutions were normally heated at a rate of 0.1 °C/min without agitation; measurements were generally taken at 500 nm. The CP was taken as the middle point of the transmittance change. DLS measurements were performed on a Malvern Zetasizer NanoZS instrument (Malvern CGS-2 apparatus) equipped with a He-Ne Laser with a wavelength of 633 nm and the scattering angle was fixed at 173°. The temperature was controlled in the range of 10-80 °C. Intensity-average hydrodynamic diameters of the dispersions were obtained by DLS through the use of non-negative least-squares (NNLS) algorithm. Disposable cuvettes were used and

the suspensions were filtered through 0.2 μm Millipore filters to remove dusts. The measurements were taken at every 1 °C after 5 minutes of equilibration time. Samples were kept at each temperature for approximately 10 minutes (equilibration + measurement time), resulting in an approximate overall heating rate of 0.1 °C/min. Aqueous solution of the copolymer for AFM measurements (5.0 g/L) was heated using the same procedure as for the CP measurements. When the temperature was raised to 45 °C, a drop of solution was deposited onto preheated silicon wafer and rapidly frozen in liquid nitrogen. The samples were freeze-dried, and kept under vacuum until the AFM measurements. The sample was imaged in air with AFM in tapping mode on a Multimode AFM with a Nanoscope IIIa controller (Digital Instruments/Veeco, Santa Barbara, CA) and silicon probes (MikroMasch U.S.A.: rectangular, no aluminum coating on tip and backside, resonance frequency 265-400 kHz, tip curvature radius <10 nm; or Nanosensors: type PPP-NCH, nominal spring constant 42 N/m, resonance frequency 330 kHz, tip radius of curvature <10 nm). The static light scattering (SLS) experiments were conducted on a CGS-3 compact goniometer (ALV GmbH) equipped with an ALV-5000 multi tau digital real time correlator at selected temperatures using a Science/Electronics temperature controller. The laser wavelength was 632 nm. The angular range was between 30 and 150° with increments of 10°. The polymer solutions (5 g/L) were filtered through a 0.2 μm filter (Millipore) directly into precleaned 10 mm tubes. The SLS experiments were conducted at 20 °C. The standard (toluene) and solvent (water) were used to calculate the Rayleigh ratio, R_v(q), and M_w.

Results and discussion

Characteristics of the polymers

The successful preparation of diblock copolymers by RAFT polymerization was demonstrated previously.^{15,17,38} Table 1 shows good agreements between the M_n measured by SEC and by NMR of the copolymers. The SEC traces of the resultant polymers are unimodal (Fig. 1) with relatively low PDI. The conversion of the monomers were monitored and remained in the range of 84-87%.

Table 1. Molecular weight and dispersity of the diblock copolymers.

Copolymer samples ^a	M _{n,NMR} ^b	M _{n,SEC} ^c	M _w /M _n ^c
PnPA ₈₄ - <i>b</i> -PEMA ₄₂	14.6 × 10 ³	13.7 × 10 ³	1.14
PnPA ₈₄ - <i>b</i> -PEMA ₈₆	19.6 × 10 ³	19.1 × 10 ³	1.15
PnPA ₄₄ - <i>b</i> -PEMA ₈₇	15.1 × 10 ³	14.6 × 10 ³	1.10

^a The subscript represents the degree of polymerization (DP) of the corresponding block. The DPs of macroinitiator PnPA were calculated from the monomer conversions determined by ¹H NMR spectroscopy and the monomer-to-initiator ratios. The DPs of PEMA were calculated from the integration ratios of the related peaks in the ¹H NMR spectra of copolymers.

^b M_{n,NMR} = [M]/[CTA]₀ × Conversion% × Molecular weight of monomer + Molecular weight of CTA.

^c Determined by SEC.

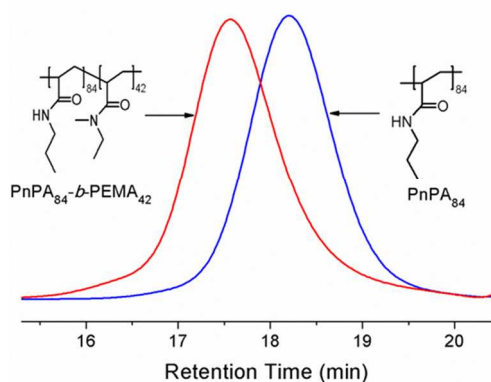


Fig. 1 SEC curves of homopolymer PnPA₈₄ and block copolymer PnPA₈₄-b-PEMA₄₂. DMF was used as the mobile phase with a flow rate of 1.0 mL/min at 50 °C and with PMMA standards.

UV-visible spectroscopy

The three diblock copolymers, PnPA₄₄-b-PEMA₈₇, PnPA₈₄-b-PEMA₈₆ and PnPA₈₄-b-PEMA₄₂, with relative PnPA to PEMA block lengths of 1 : 2, 1 : 1 and 2 : 1, underwent multiple transitions at elevated temperatures in water (Fig. 2A), but they show different transition and aggregation behaviors, despite their structural similarity. PnPA₈₄-b-PEMA₄₂ and PnPA₄₄-b-PEMA₈₇ exhibit two CPs during heating, while the solution of PnPA₈₄-b-PEMA₈₆ became relatively clear after the first CP, and remained so until the end of heating process, suggesting the absence of the second CP. These differences should be a result of the relative sizes of the two blocks. Both PnPA₈₄-b-PEMA₈₆ and PnPA₈₄-b-PEMA₄₂, having the same PnPA block length, show a similar first CP but different changes in transmittance. This indicates that the aggregation at first CP is mainly related to the size of the PnPA block in the copolymers. At their first CPs, the turbidity of solutions of the block copolymers follows the ascending order of PnPA₄₄-b-PEMA₈₇, PnPA₈₄-b-PEMA₈₆ and PnPA₈₄-b-PEMA₄₂. PnPA₄₄-b-PEMA₈₇ showed a higher first CP than the other two copolymers, likely caused by a more significant effect of the relatively more hydrophilic PEMA block on a shorter PnPA block.^{15,16,39,40}

For PnPA₈₄-b-PEMA₄₂ and PnPA₄₄-b-PEMA₈₇, the two CPs correspond to the individual CPs of the homopolymers, PnPA and PEMA (22 °C and 56-57 °C, respectively),^{34,35} and therefore reflect the successive collapsing of the PnPA and PEMA blocks in the copolymers.¹⁴ The deviation of the CPs of the copolymers from those of the homopolymers is a result of the mutual influence of the relative hydrophilicity of two individual blocks linked covalently.²³ In this work, we have selected PnPA₈₄-b-PEMA₄₂ for most of the following experiments.

Fig. 2B shows the effect of concentration on the transmittance of the aqueous solution of PnPA₈₄-b-PEMA₄₂ as a function of temperature during heating. The solutions of different concentrations exhibit different transition characteristics. When the concentration is lower than 3 g/L, the thermosensitivity of PnPA₈₄-b-PEMA₄₂ corresponds to a two-step collapse process, which is similar with what was observed for PnPA-b-PiPA.¹⁵ When the concentration is between 3 and 9.5 g/L, two CPs were observed, showing two soluble-insoluble transitions. For instance, a 5 g/L solution of PnPA₈₄-b-PEMA₄₂ was clear at low temperature and turned cloudy at 25 °C due to the formation of large aggregates. The size of the aggregates

formed is affected by the heating rate and the solution is less turbid at a higher heating rate (Fig. S2A). The cloudy mixture remained stable at 32 °C and no obvious change was observed after 24 h for the transmittance of the mixture and for the diameter of the aggregates determined by DLS. This indicates the formation of the large aggregates at the first CP is a thermodynamically-controlled process. However, the solution became clear again when heated to a higher temperature. The solution remained clear until it became turbid again at 60 °C. Only one CP was observed at a concentration higher than 9.5 g/L, corresponding to the phase transition of the PnPA block.

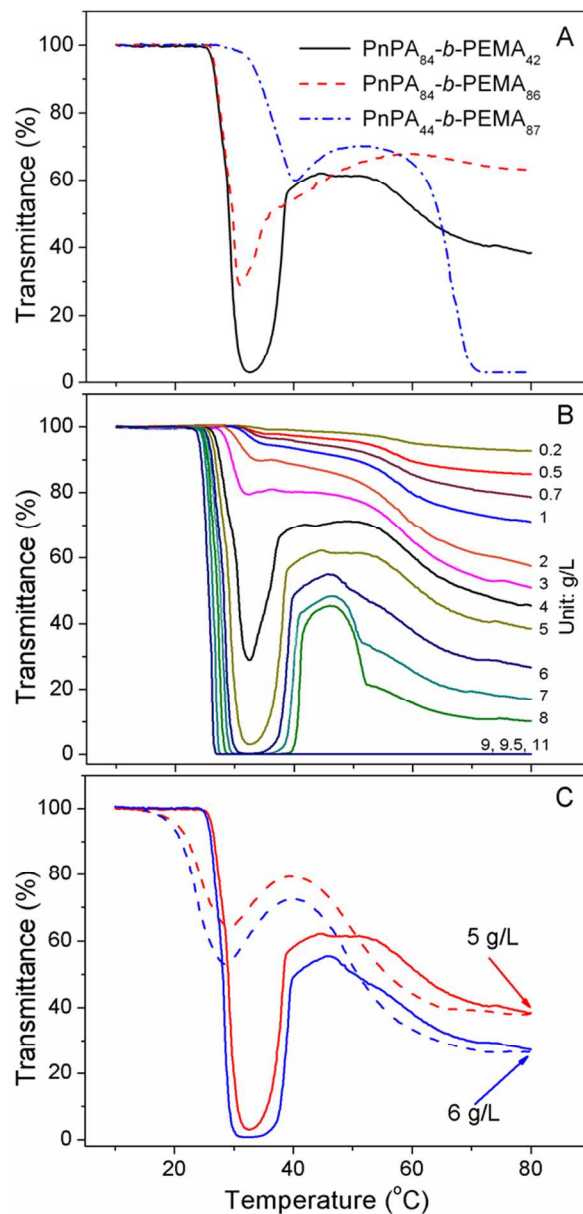


Fig. 2 Transmittance of aqueous solutions of diblock copolymers as a function of temperature observed at 500 nm with a heating rate of 0.1 °C/min. (A) PnPA₈₄-b-PEMA₄₂, PnPA₈₄-b-PEMA₈₆ and PnPA₄₄-b-PEMA₈₇, polymer concentration 5 g/L; (B) PnPA₈₄-b-PEMA₄₂ at different concentrations; (C) PnPA₈₄-b-PEMA₄₂ (5.0 and 6.0 g/L) with a heating (solid) or cooling (dashes) rate of 0.1 °C/min.

This seemingly complex thermally-induced process is reversible with a certain hysteresis (Fig. 2C). Temperature was the only factor determining the state of the solution. The hysteresis can be ascribed to the additional interchain hydrogen bonding formed in the collapsed state at higher temperatures, which has been extensively studied by Wu and co-workers for aqueous solutions of PiPA.⁴¹ However, the transmittance of the polymer during cooling was much higher than that determined during heating around the first CP, suggesting that it is rather difficult to form large aggregates during the cooling process.

Light scattering studies

The phase transitions of these diblock copolymers were further studied by DLS. Fig. 3 shows the comparison of the change in the hydrodynamic diameters (D_h) and transmittance as a function of temperature for the PnPA₈₄-*b*-PEMA₄₂ solution. The effect of polymer concentration is significant in the aggregation of the polymer. At a higher polymer concentration (5 g/L, Fig. 3A), D_h values remain smaller than 10 nm,

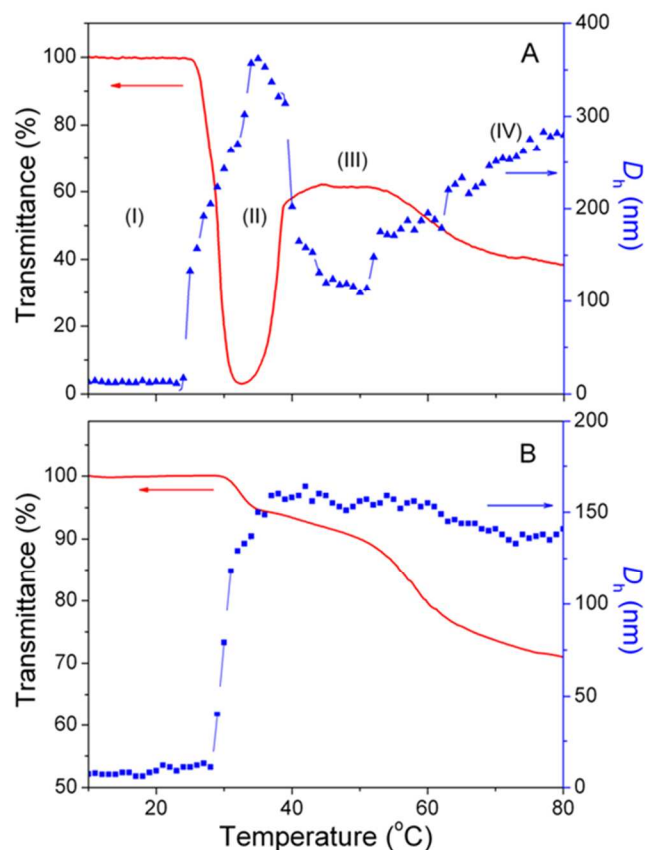


Fig. 3 Comparison of intensity-average size distribution (D_h) and transmittance of PnPA₈₄-*b*-PEMA₄₂ as a function of temperature at concentrations of (A) 5 g/L; (B) 1 g/L.

sometimes up to 14 nm below 24 °C in the case of intensity-average size distribution. However, the D_h values become < 7 nm in the case of number-average size distribution. For example, Fig. S3A shows that the solution of PnPA₈₄-*b*-PEMA₄₂ exhibits two distinct intensity size distributions at 20 °C. The dominant peak is observed at around 6 nm, while the other peak is ascribed to the scattering of larger aggregates. The number-average size distribution of solution shows monomodal distribution (Fig. S3B), with a D_h value of 3.4 nm, since larger particles scatter much more light than smaller ones

($I \propto r^6$), a peak with a high intensity can be caused by fewer particles. Therefore, these results indicate that the polymer is dissolved and exists mostly as individual molecules at such low temperatures and low concentrations. As shown in Fig. 3A, when the temperature was raised to 25 °C, D_h increased dramatically to > 150 nm and up to a maximum 370 nm at 34 °C, indicating that the polymer solution underwent a phase separation. At ca. 40 °C, D_h showed a sharp decrease to ca. 110 nm and the solution became quite clear again. Large aggregates were observed again above 60 °C. At a lower concentration (1 g/L, Fig. 3B) no change in size was observed in the range of 10–28 °C ($D_h < 10$ nm), but D_h increased dramatically when the temperature increased beyond 29 °C, up to 160 nm at 38 °C, followed by a gradual decrease in D_h . A very concentrated solution (10 g/L) showed a similar trend ($D_h < 13$ nm below CP) to that of a low concentration, with a CP at a lower temperature (21.5 °C, Fig. S4).

The aggregation process

On the basis of results discussed above, a mechanism is proposed for the thermally-induced phase transition of PnPA₈₄-*b*-PEMA₄₂ showing two CPs (Fig. 4A). Firstly, the diblock copolymers dissolved in water as unimers below their first phase transition temperature (CP₁) (Fig. 4A-I). When the solution was heated to the CP₁, the PnPA block began to dehydrate due to the disruption of hydrogen bonds with water,⁴² with a simultaneous formation of micellar clusters (Fig. 4A-II). This is attributed to the relative short hydrophilic PEMA block in the copolymer, which may not be sufficiently long to stabilize isolated micelles, and/or may not favor the formation of individual micelles with high curvature. The need of relative long hydrophilic block versus the size of the hydrophobic block to provide stable micelles in the case of non-ionic amphiphilic block copolymers was reported before.^{14,43,44} At the beginning of the first thermal transition, a part of the PnPA block before dehydration may form intra- and interchain hydrogen bonds with the PEMA block, since the PnPA and PEMA blocks are a pair of hydrogen-bonding donor and acceptor. This interaction will also promote the formation of micellar clusters, which exist as insoluble complexes. Mori et al also found that around the first transition temperature, the cooperative dehydration of the first poly(*N*-acryloyl-L-proline methyl ester) block led to the simultaneous formation of the intra- and interchain hydrogen bonds between the carboxyl and hydroxyl groups in the second poly(*N*-acryloyl-4-*trans*-hydroxy-L-proline) block with the amide and ester groups in first block to afford insoluble aggregates.²⁰ Increasing the temperature led to further dehydration of the PnPA block, which promoted the shrinkage of the core formed by the dehydrated PnPA block, so that the PEMA block became sufficiently long to stabilize the isolated micelles. The intra- and interchain hydrogen bonds between the PnPA and PEMA blocks dissociated because of the greater mobility of the copolymer chains at higher temperatures.²⁰ Therefore, these micellar clusters restructured and dissociated into smaller micelles with a dehydrated PnPA core and a water-soluble PEMA shell, leading to an optically clear solution (Fig. 4A-III). At even higher temperatures, both PnPA and PEMA blocks became hydrophobic, forming large aggregates and thus showing a second cloud point, CP₂ (Fig. 4A-IV). It is to be noted that the copolymer PnPA₄₄-*b*-PEMA₈₇ shows a very similar concentration-temperature phase diagram (Fig. S7).

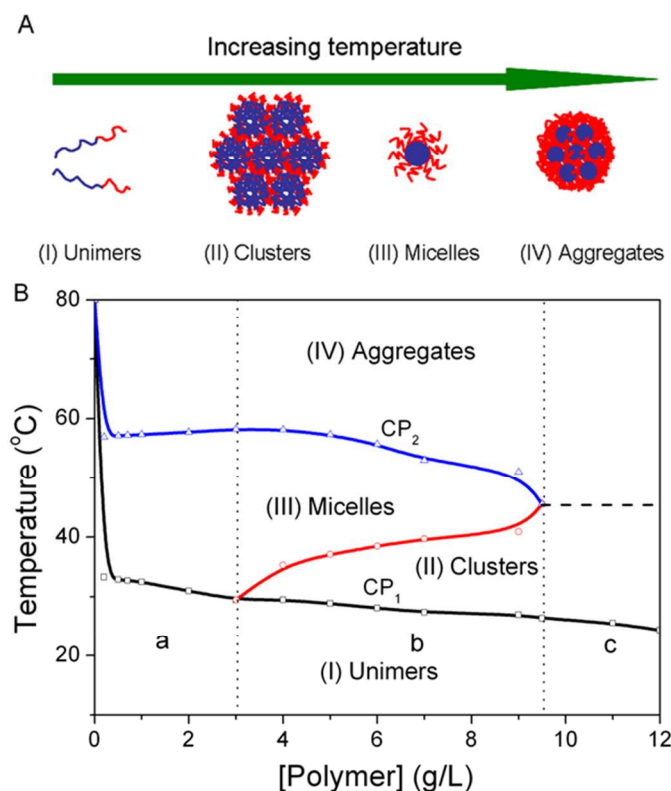


Fig. 4 (A) Illustration of the morphology of the self-assembled structures of PnPA₈₄-b-PEMA₄₂, showing the transformation of unimers into micellar clusters and then into micelles, and further into aggregates with increasing temperature. (B) Concentration-temperature phase diagram of PnPA₈₄-b-PEMA₄₂. Low concentration range a: Unimers change into micelles and then to aggregates; Medium concentration range b: Unimers transform into micellar clusters and then into micelles and further into aggregates; High concentration range c: The unimers transform into clusters and into aggregates with increasing temperature. The concentration and temperature scales are approximate and serve as a general trend.

Table 2. Characteristics of PnPA₈₄-b-PEMA₄₂ aggregates in 5.0 g/L aqueous solutions at two different temperatures as studied by SLS.

Temperature (°C)	M_w (g/mol)	N_{agg}^a	R_g (nm)
32	5.12×10^7	3.07×10^3	112
45	1.00×10^7	6.01×10^2	52

^aAggregation number calculated from M_w of the micelles and of the polymers

Since the micellar clusters formed by PnPA₈₄-b-PEMA₄₂ are split into the micelle-like structures, it is also possible to examine the dissociation process of the micellar clusters by SLS (Figure 5A). At 32 °C, large aggregates with weight-average mass $M_w \approx 5.12 \times 10^7$ and $R_g = 112$ nm are formed (Table 2). When the temperature is raised to 45 °C, the molar mass of the associated structures is decreased by 5 times to $M_w \approx 1.00 \times 10^7$, confirming that the dissociation or fragmentation of the large structures formed at 32 °C. The aggregation

number N_{agg} also decreases by 5 times from 3.07×10^3 to 6.01×10^2 in the same temperature range (Table 2). In the meantime, the radius of gyration R_g also decreases from ca. 112 to 51 nm and the ratio of the radius of gyration to hydrodynamic radius is $R_g/R_h \approx 0.93$. This is in good agreement with spherical micelles that usually have a value of R_g/R_h in the range 0.8-1.0.⁴⁵

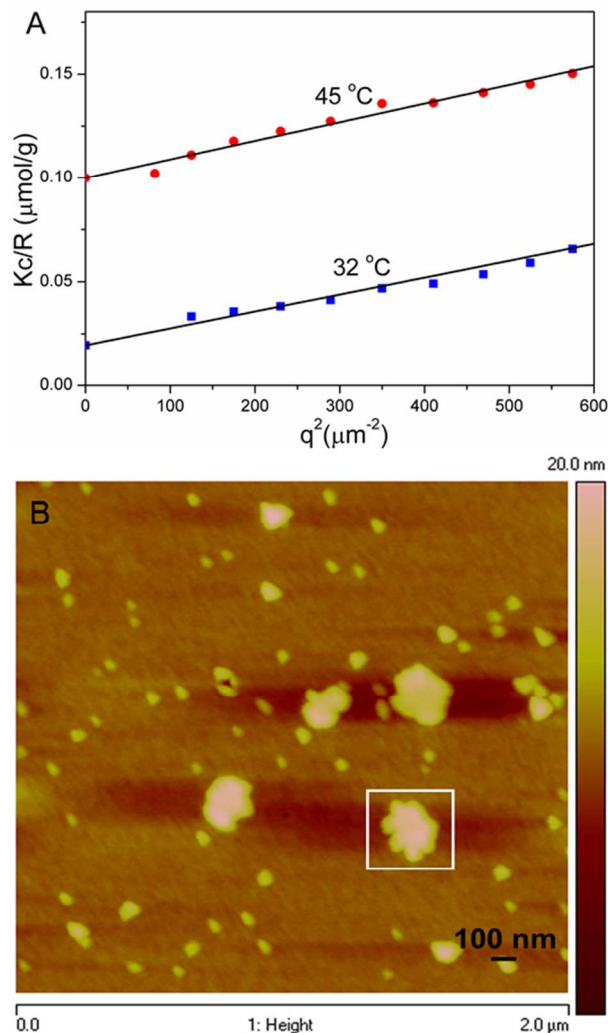


Fig. 5 (A) Data obtained from static light scattering (SLS) for PnPA₈₄-b-PEMA₄₂ (5.0 g/L) in water at 32 and 45 °C, respectively, where the intercepts with the y-axis yielded $1/M_w$. (B) AFM topography images (height mode) of PnPA₈₄-b-PEMA₄₂, the sample was prepared by dropping a aqueous solution (5.0 g/L, 45 °C) onto silicon wafer and rapidly frozen using liquid nitrogen. The samples were freeze-dried before measurements.

AFM was also employed to visualize the dissociation of the micellar clusters. The AFM images of PnPA₈₄-b-PEMA₄₂ (Fig. 5B) show the major population of small aggregates of about 70 nm in diameter, which coexist with a few large aggregates of about 300 nm in diameter. Here, the size of the small aggregates observed by AFM is smaller than the average hydrodynamic diameter measured by DLS (ca. 110 nm), which may be an effect of drying.⁴⁶ More importantly, the large aggregates show a secondary structure after a closer look at the image (the square in Fig. 5B). These large aggregates are

composed of smaller aggregates. The major population observed by AFM is probably the micelles formed by the dissociation of the loose clusters. At the beginning of dehydration of the PnPA block, a loose core-shell micellar structure may form and the relatively short PEMA block cannot provide enough stabilization for the core, leading to the formation of the micellar clusters. This structure may be different from those of the aggregates at the first CP observed by Hoogenboom et al, where the aggregates are associated structures of polymer chains.²⁴

From PnPA₈₄-*b*-PEMA₄₂ to PnPA₈₄-*b*-PEMA₈₆ and to PnPA₄₄-*b*-PEMA₈₇, with increasing ratio of the PEMA to PnPA blocks from 1 : 2 to 1 : 1 and to 2 : 1, the formation of the micellar clusters and the appearance of the first CP become less abrupt due to the efficient stabilization of the PnPA core by the longer more hydrophilic PEMA block. In the case of PnPA₈₄-*b*-PEMA₈₆ (1 : 1), after the loose clusters dissociated into smaller micelles, the second thermal transition may cause the dehydration of the shell, but the second CP is not clearly observed. This phenomenon has often been observed for thermoresponsive block copolymers, and typically discussed in the context of mesoglobule formation.^{14,47,48} In the case of PnPA₄₄-*b*-PEMA₈₇, the formation of loose clusters is less favored due to the presence of a longer PEMA block, but the second CP was observed, showing a similar transition as PnPA₈₄-*b*-PEMA₄₂ (Figs. S6 and S7).

Phase diagram

Based on the results of PnPA₈₄-*b*-PEMA₄₂ discussed above, we have drawn a phase diagram of the transitions as shown in Fig. 4B. When the concentration is low (< 3 g/L, Fig. 4B-zone a), the polymer molecules firstly self-assemble into micelles due to the dehydration of the PnPA block with increasing temperature. The low concentration of the polymers prevents the formation of micellar clusters. Then the dehydration of the PEMA block of the polymer leads to large aggregates above the CP of the PMEA block. At intermediate concentration range (3~9.5 g/L, Fig. 4B-zone b), the dehydration of the PnPA block and the hydrogen bonding between the PnPA and PEMA blocks lead to the formation of micellar clusters, showing CP₁. With increasing temperature, these clusters of micelles restructure and dissociate into smaller micelles, making the solution clear again. At higher temperature, even the PEMA block starts to dehydrate, causing the formation of large aggregates at CP₂. When the polymer concentration is high (> 9.5 g/L, Fig. 4B-zone c), only one CP was observed, indicating the formation of micellar clusters was followed closely by further dehydration to form large aggregates. The main differences between the loose clusters and aggregates are in their structures; the aggregates are more compact than the loose clusters due to their dehydration (Fig. 4A). Therefore, it is not easy to draw a clear boundary between the area of loose clusters and more compact aggregates in Figure 4B-zone c (dashes).

Unusual aggregation behaviors of PiPA₈₈-*b*-poly(*N*-acryloyl pyrrolidine)₁₉₇ were also observed by Laschewsky et al, where the transmittance was partially reduced in the temperature range between the two CPs of the two homopolymers and passed through a local minimum, suggesting a two-step aggregation process.¹⁹ All the data to date^{18,19,23,24,49} provide indications of the required characteristics of the block copolymers showing the complex thermoresponsive behavior in Fig. 4B: (1) the relatively short length of the block with a higher CP may lead to the micellar clusters; (2) the interaction between the two blocks during the dehydration of the block with a lower CP

may facilitate the formation of loose aggregates or clusters; (3) the difference of the two CPs should be large enough to allow the dissociation of the loose clusters into micelles.

Conclusions

The block copolymers of PnPA-*b*-PEMA synthesized in this study with a suitable ratio of the PnPA to PEMA blocks showed two CPs in aqueous solutions and complex thermoresponsive properties. The solution changes from a transparent, to a cloudy, then to a clear and finally to a turbid liquid with increasing temperature. This may be explained by the relative length and thermosensitivity of the individual blocks. The first CP is associated with the transition from unimers to loose micellar clusters. These clusters may dissociate into smaller micelles with increasing temperature. At the second CP, the smaller micelles form more compact aggregates, leading to a turbid liquid. The relative block length and the hydrogen bonding between the blocks play a decisive role in the formation and dissociation of the micellar clusters. The thermoresponsive behavior may vary as a consequence. The understanding of the complex aggregation properties of such polymers provides insights and guidelines towards the rational design of thermoresponsive copolymers exhibiting interesting physico-chemical properties and enlarges the repertoire of functional materials.

Acknowledgements

Financial support from NSERC of Canada, FQRNT of Quebec, and the Canada Research Chair program is gratefully acknowledged. Authors are members of CSACS funded by FQRNT and GRSTB funded by FRSQ. The authors thank Dr. Zhida Wang for his help with the AFM measurements and Mr. Sylvain Essiembre and Mr. Pierre Ménard-Tremblay for their technical support. The authors also thank Prof. F. M. Winnik and Dr. E. Korchagina for their help with the SLS experiments.

Notes and references

Département de chimie, Université de Montréal, C. P. 6128, Succursale Centre-ville, Montreal, QC, H3C 3J7, Canada

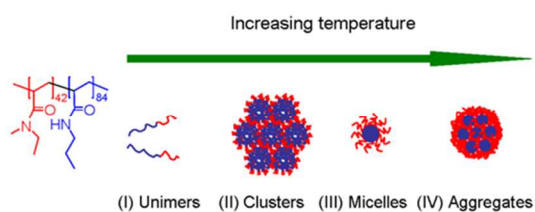
Electronic Supplementary Information (ESI) available: [¹H NMR spectrum of the copolymer. Transmittance versus temperature plots with a different heating rates and wavelengths. DLS measurements. Transmittance versus temperature plots of PnPA₄₄-*b*-PEMA₈₇ at different concentrations]. See DOI: 10.1039/b000000x/

- 1 E. S. Gil and S. M. Hudson *Prog. Polym. Sci.* 2004, **29**, 1173.
- 2 S. Aoshima and S. Kanaoka *Adv. Polym. Sci.* 2007, **210**, 169.
- 3 S. Ganta; H. Devalapally; A. Shahiwala and M. Amiji *J. Control. Release* 2008, **126**, 187.
- 4 A. Kumar; A. Srivastava; I. Y. Galaev and B. Mattiasson *Prog. Polym. Sci.* 2007, **32**, 1205.
- 5 C. Alarcón; H. de las; S. Pennadam and C. Alexander *Chem. Soc. Rev.* 2005, **34**, 276.
- 6 A. Kikuchi and T. Okano *Prog. Polym. Sci.* 2002, **27**, 1165.

- 7 D. Schmaljohann *Adv. Drug Deliver. Rev.* 2006, **58**, 1655.
- 8 C. Weber; R. Hoogenboom and U. S. Schubert. *Prog. Polym. Sci.* 2012, **37**, 686.
- 9 Z. Shen; B. Shi; H. Zhang; J. Bi and S. Dai *Soft Matter* 2012, **8**, 1385.
- 10 S. Aluri; M. K. Pastuszka; A. S. Moses; J. A. MacKay *Biomacromolecules* 2012, **13**, 2645.
- 11 Pietsch, C.; Schubert, U. S. and Hoogenboom, R. *Chem. Commun.* 2011, **47**, 8750.
- 12 I. Berndt; J. S. Pedersen and W. Richtering *J. Am. Chem. Soc.* 2005, **127**, 9372.
- 13 A. Kjøniksen; K. Zhu; G. Karlsson and B. Nyström *Colloids and Surf., A*: 2009, **333**, 32.
- 14 J. Weiss; C. Böttcher and A. Laschewsky *Soft Matter* 2011, **7**, 483.
- 15 Y. Cao; N. Zhao; K. Wu; X. X. Zhu *Langmuir* 2009, **25**, 1699.
- 16 D. Xie; X. Ye; Y. Ding; Zhang, G.; Zhao, N.; Wu, K.; Cao, Y. And Zhu, X. X. *Macromolecules* 2009, **42**, 2715.
- 17 Y. Cao; X. X. Zhu; J. Luo and H. Liu *Macromolecules* 2007, **40**, 6481.
- 18 X. Han; X. Zhang; Q. Yin; J. Hu; H. Liu and Y. Hu *Macromol. Rapid Comm.* 2013, **34**, 574.
- 19 M. Mertoglu; S. Garnier; A. Laschewsky; K. Skrabania and J. Storsberg *Polymer* 2005, **46**, 7726.
- 20 H. Mori; I. Kato; S. Saito and T. Endo *Macromolecules* 2010, **43**, 1289.
- 21 Zhang, Q.; Hong, J.-D. and Hoogenboom, R. *Polym. Chem.* 2013, **4**, 4322.
- 22 J. Weiss and A. Laschewsky *Macromolecules* 2012, **45**, 4158.
- 23 F. J. Hua; X. G. Jiang and B. Zhao *Macromolecules* 2006, **39**, 3476.
- 24 L. T. T. Trinh; H. M. L. Lambermont-Thijs; U. S. Schubert; R. Hoogenboom and A.-L. Kjøniksen. *Macromolecules* 2012, **45**, 4337.
- 25 C. Tsitsilianis *Soft Matter* 2010, **6**, 2372.
- 26 H. G. Schild *Prog. Polym. Sci.* 1992, **17**, 163.
- 27 J. E. Chung; M. Yokoyama; M. Yamato; T. Aoyagi; Y. Sakurai and T. Okano *J. Control. Release* 1999, **62**, 115.
- 28 H. Wei; X.-Z. Zhang; Y. Zhou; S.-X. Cheng and R.-X. Zhuo *Biomaterials* 2006, **27**, 2028.
- 29 S. Choi; B.-C. Choi; C. Xue and D. Leckband *Biomacromolecules* 2013, **14**, 92.
- 30 H. Y. Liu and X. X. Zhu *Polymer* 1999, **40**, 6985.
- 31 S. Luo; J. Xu; Z. Zhu; C. Wu and S. Liu *J. Phys. Chem. B* 2006, **110**, 9132.
- 32 J. Weiss; A. Laschewsky *Langmuir* 2011, **27**, 4465.
- 33 M. Savoji; S. Strandman and X. X. Zhu *Macromolecules* 2012, **45**, 2001.
- 34 D. Ito and K. Kubota *Macromolecules* 1997, **30**, 7828.
- 35 S. Ito *Kobunshi Ronbunshu* 1989, **46**, 437.
- 36 K. J. Shea; G. J. Stoddard; D. M. Shavelle; F. Wakui and R. M. Choate *Macromolecules* 1990, **23**, 4497.
- 37 J. T. Lai; D. Filla and R. Shea *Macromolecules* 2002, **35**, 6754.
- 38 G. Moad; E. Rizzardo and S. H. Thang *Aust. J. Chem.* 2005, **58**, 379.
- 39 K. Skrabania; J. Kristen; A. Laschewsky; O. Akdemir; A. Hoth and J.-F. Lutz *Langmuir* 2007, **23**, 84.
- 40 Y. Maki; H. Mori and T. Endo *Macromol. Chem. Phys.* 2010, **211**, 45.
- 41 H. Cheng; L. Shen and C. Wu *Macromolecules* 2006, **39**, 2325.
- 42 X.-C. Yin and H. D. H. Stöver *Macromolecules* 2002, **35**, 10178.
- 43 S. Garnier and A. Laschewsky *Langmuir* 2006, **22**, 4044-4053.
- 44 S. Garnier and A. Laschewsky *Colloid Polym. Sci.* 2006, **284**, 1243.
- 45 Xie, D.; Xu, K.; Bai, R. and Zhang, G. *J. Phys. Chem. B* 2007, **111**, 778.
- 46 N. G. Khlebtsov *Colloid J.* 2003, **65**, 652.
- 47 V. Aseyev; H. Tenhu and F. Winnik *Adv. Polym. Sci.* 2006, **196**, 1.
- 48 P. Kujawa; V. Aseyev; H. Tenhu and F. Winnik *Macromolecules* 2006, **39**, 7686.
- 49 R. Longenecker; T. Mu; M. Hanna; N. A. D. Burke and H. D. H. Stöver *Macromolecules* 2011, **44**, 8962.

For Table of Contents Use Only

Complex Thermoresponsive Behavior of Diblock Polyacrylamides

*Y-G. Jia, X. X. Zhu**

A phase diagram is drawn for complex thermoresponsive transitions of diblock copolymers from unimers to micellar clusters, micelles and aggregates.